

Passive subduction of the Phoenix plate remnant at the South Shetland trench, Antarctic Peninsula

B. Della Vedova,¹ F. Accaino,² M. F. Loreto,² and U. Tinivella²

¹Dipartimento di Ingegneria Civile e Ambientale (DICA), Università di Trieste, Via Valerio 10, 34127 Trieste, Italy (dellavedova@units.it)

²Istituto Nazionale di Oceanografia e Geofisica Sperimentale (OGS) - Trieste, Italy (faccaino@ogs.trieste.it).

Summary We present multibeam bathymetry, Chirp profiles and seismic data acquired in the South Shetland Trench during the Antarctic summer 2003-2004 (R/V OGS-Explora cruise), to study the differential passive subduction affecting the Phoenix Plate remnant, subdivided into three main segments by the “D” and “E” Fracture Zones. The investigated area (160 x 60 km) includes parts of the trench, incoming oceanic plate and outer front of the Antarctic Peninsula accretionary prism. The integrated dataset displays an interesting faults pattern deforming the seafloor and oceanic crust with variable orientation, controlled by the slab pull down and by the fracture zones which act as effective mechanical discontinuities. The differential mechanical coupling across the Hero, Shackleton, “E” and “D” Fracture Zones influences the regional stress field distribution and the sinking of the oceanic segments, during passive subduction and roll-back.

Citation: Della Vedova B., Accaino F., Loreto M.F., Tinivella U. (2007), Passive subduction of the Phoenix plate remnant at the South Shetland trench, Antarctic Peninsula, *in* Antarctica: A Keystone in a Changing World – Online Proceedings of the 10th ISAES X, edited by A.K. Cooper and C.R. Raymond et al., USGS Open-File Report 2007-1047, Extended Abstract 084, 4 p.

Introduction

The passive subduction of oceanic lithosphere is an interesting case of study, because the pull-down forces of subducting oceanic slabs still continue to occur, even when active spreading, at the mid ocean ridge, ceases. This change in stress regime at convergent margins induces a regional tectonic relaxation in the subduction trench and in the back-arc areas.

The extension affecting the retreating oceanic plate is mainly represented by normal faults, associated to horst and graben structures (Masson, 1991). These structures were observed along the northern Chilean margin (Scholl et al., 1970; Carbotte and Macdonald, 1994) and along the Japan trench (Kobayashi et al., 1998), with variable orientation with respect to the margin strike (Kobayashi et al., 1998; von Huene and Ranero, 2003). Because of this regional relaxation, the mechanical response of the oceanic plate, segmented by transform faults, could laterally change due to the different age and physical properties pertaining to each subducting lithospheric segment.

The Phoenix plate (PHO) is the last remnant of the Nazca plate subduction beneath of the Antarctic (ANT) plate (Barker, 1982; Larter and Barker, 1991). Despite cessation of spreading at the ANT-PHO ridge, recent seismic events recorded within the fore-arc region of the South Shetland (Robertson Maurice et al., 2003) indicate that subduction is still active. The surface projection of the subducted Hero and Shackleton fracture zones, laterally confining the PHO plate, are also delimiting the lateral extent of the Bransfield microplate (Lawver et al., 1995), which is separated from the Antarctic Peninsula (AP) by the opening of the Bransfield Strait back-arc basin. Passive subduction at the South Shetland trench is characterized by: 1) an angle of incidence that progressively decreases from orthogonal, moving from the Hero towards the Shackleton FZ; 2) bending and roll-back of the oceanic plate due to cessation of the ANT-PHO spreading ridge; 3) extensional regime in the incoming oceanic plate; 4) opening of the Bransfield Strait back-arc basin. The PHO remnant is subdivided into 3 main segments (Barker, 1982) by the “D” and “E” Fracture Zones (FZ) (Fig. 1a). The age of the lithosphere increases from 14 Ma (to the SW) to about 23 Ma (to the NE), according to magnetic chrons identification (Larter and Barker, 1991). Each segment is characterized by different properties, such as: thickness, density, elastic thickness and rigidity. These differences are also recorded by the (i) lateral variability of the trench and prism morphology, (ii) plate tectonic setting (Kim et al., 1995), (iii) sediment blanketing, (iv) deformation of the continental margin and (v) associated magmatism (Hawkes, 1981). In particular, differences in the strain pattern should be expected across the subducting oceanic segments. In order to test these hypotheses in the study area (Fig. 1a), an integrated geophysical cruise was performed during the Antarctic summer 2003-2004, onboard R/V OGS-Explora, as part of the Program SLAPPSS (Subduction of the LAsT Phoenix Plate Segments beneath the South Shetland margin, Antarctic Peninsula), supported by the Italian Programma Nazionale di Ricerche in Antartide (PNRA). The geophysical dataset is composed by high-resolution multibeam bathymetry, Chirp profiles, gravity and magnetic measurements, reflection and refraction (Ocean Bottom Seismometer) seismic data. Here we present crustal and sedimentary structures of the oceanic segments, as imaged by Multibeam bathymetry, Chirp profiles and seismic reflection data.

The study of the last PHOenix (PHO) plate segment offers the opportunity to study the final passive subduction of a locked oceanic plate remnant and its relationship on the opening of the Bransfield Strait back-arc basin.

Data acquisition and processing

Multibeam bathymetry

High-resolution bathymetry was acquired using the Seabat 8150 multibeam system mounted on the OGS-Explora, with a

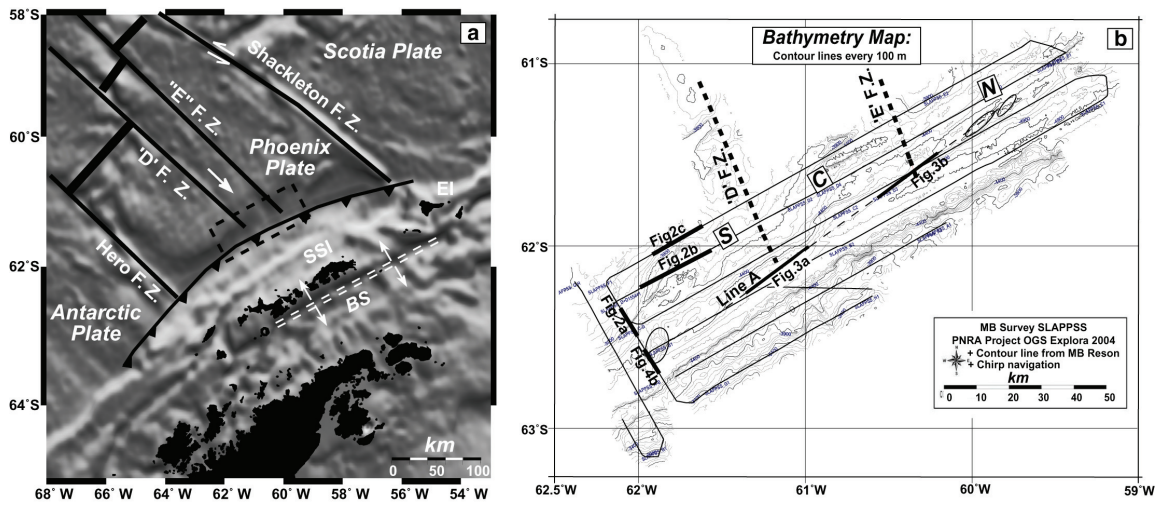


Figure 1. a: Index map of the area (from Sandwell and Smith, 1997). The dashed rectangle indicates the study area; the single arrow is the direction of subduction; three oceanic segments are defined by “D” and “E” FZ. EI: Elephant Island; SSI: South Shetland Island; BS: Bransfield Strait. b: High resolution bathymetric map (Multibeam image) of the investigated area. S=Southern; C=Central; and N=Northern segments. Thin lines indicate Chirp profiles; thick black lines indicate portions of Chirp and seismic profiles shown in Figures 2 and 3. Ellipses border morphological highs.

nominal depth range of 15 km and a frequency of 12 kHz. The swath coverage was about 10 km, corresponding to 2.5 times the water depth. Data acquisition and processing was performed using the PDS2000 software. Sea water velocity was measured by 4 CTD probes in the water column. Horizontal resolution is 150 m, whereas the vertical one is about 20 m. The investigated box (9700 km²) was covered by seven swaths parallel to the trench axis (Fig. 1b). Water depth exceeds 5000 m.

Chirp sub-bottom profiles

About 1000 km of Chirp profiles were acquired, using the CAP-6600 Chirp II, with 16 transducer and 2-7 kHz of sweep. Chirp profiler provides instantaneous amplitude records, that allow image processing of the data. The sampling rate was 0.533 ms and the error was in the order of one meter. The images were processed using the Seismic Unix (Cohen and Stockwell, 2003). Despite the low quality of Chirp data, several important discontinuities were recognized (Fig. 2).

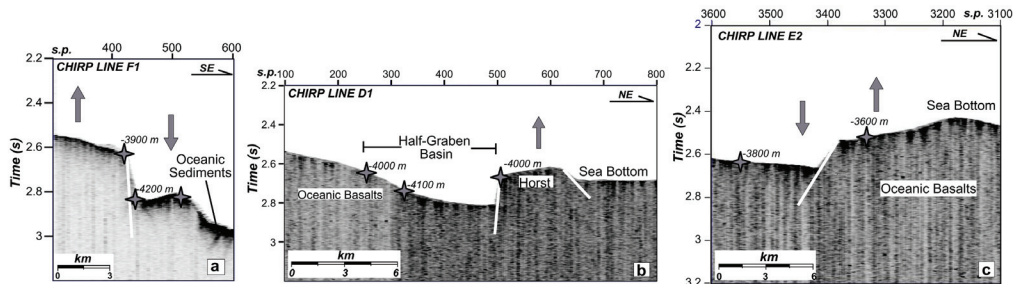


Figure 2. a: Chirp line F1. Thick arrows indicate relative movements of faulted oceanic crust; the maximum throw of the seafloor is about 320 m. b: Chirp line D1; the maximum throw is about 220 m. c: Chirp profile E2; maximum vertical offset is about 180 m. See location in Fig. 1b.

Multichannel seismic reflection data

One Multichannel Seismic line (MCS) only was acquired parallel to the trench (Fig. 1b) using a 600 m long streamer, 48 channels and group interval of 12.5 m. The seismic source was two sub-arrays of eight sleeve guns each, for a total volume of 2160 cu. in., air pressure of 140 bars and 100 m shot interval. The recording length was 20 s and sampling rate 2 ms. Standard seismic data processing was performed, including post-stack time migration (Fig. 3a and b). Processing was performed using Seismic Unix.

Discussion

The multibeam bathymetry, Chirp and seismic data allow to recognize the main features of the the incoming oceanic crust, South Shetland trench and frontal AP accretionary prism. To better analyse the structural setting of the PHO plate remnant we identify the three oceanic segments (Fig. 1b) as Southern, Central and Northern segment, respectively.

The bathymetry of the oceanic domain across the three segments (at about the same distance from the trench) shows a regional pattern characterized by the greatest depth in the central segment, with slightly decreasing depths moving towards the adjacent segments. This observation is confirmed by previous studies (Lodolo et al., 2002; Kim et al., 1995) and reflects, with local differences, the top of the oceanic crust entering the subduction zone (see Fig. 3). The Southern and Northern segments are interested by normal faults, with vertical offsets up to about 200 m (Fig. 2), forming significant oblique lineaments with respect to the trench and plate bending axes. These two segments are characterized by a shallower and rougher seafloor morphology, as compared to the Central segment, characterized by a single ridge parallel to the trench axis, likely corresponding to the oceanic peripheral bulge. These structural features affect also the sediment deposits (Fig. 3a). The stress field affecting the subducting oceanic plate changes from one segment to the other, across the “D” (Fig. 3a) and “E” (Fig. 3b) FZs, which seem to be characterized by a weak coupling. MCS data show a variable sediment blanketing on top of the oceanic basement, with strong lateral changes. Clear elongated asymmetric basins correspond to the “D” and “E” FZs and to their post early Miocene evolution. Crustal reflectors are going to be integrated with OBS data.

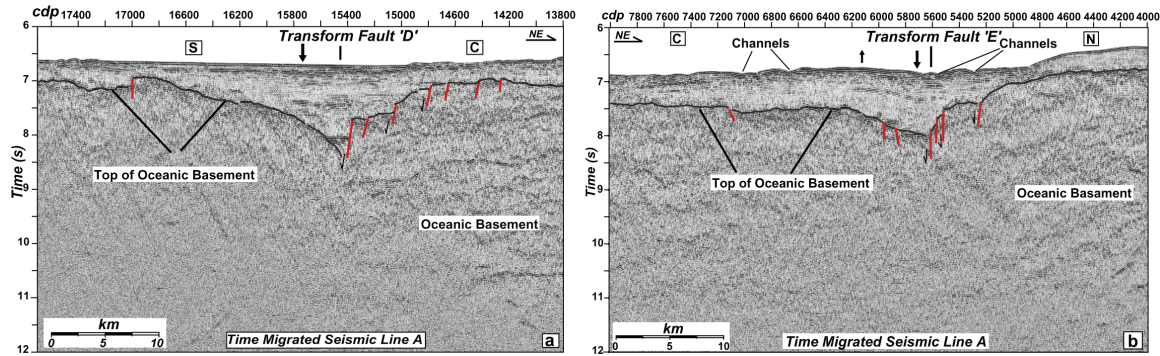


Figure 3. a: Post-stack time migrated MCS line A, crossing the “D” FZ. b: MCS line A, crossing the “E” FZ (See location in Fig. 1b). S indicates the Southern, C the Central and N the northern segment of the PHO plate, respectively.

The irregular morphology of the trench ocean-ward (Figs. 1b and 4) is locally controlled by the recent oblique fault pattern, as suggested by its sharp bends in correspondence with these lineaments, by the “D” and “E” FZs, that favour the differential sinking, and by the northward regional trench widening. The oceanic crust to the south is younger and, apart from the mechanical coupling, it should exhibit a shallower depth. The trench in the Southern segment is narrower and shallower than in the Northern one due to: (i) the different age of the crust, (ii) the relative movements along the lateral plate boundaries (Hero and Shackleton FZs) and (iii) to oceanic roughness. The morphology of the outer deformation front, represented by elongated ridges and small lobes and narrow canyons crosscutting the frontal accretionary wedge (Fig. 4), is

likely controlled by the structural elements of the subducting plate (Loreto et al., 2006).

The joint analysis of the bathymetric and seismic data recognises a structural pattern of normal faults affecting the PHO plate; they are obliquely oriented with respect to the “E” and “D” FZs and are associated to horst and graben structures. The FZs are clearly imaged on the seismic section (Fig. 3), as a 5-10 km wide V-shape depressions of the oceanic basement, with maximum depth up to 1 s twt. The basement here is interested by intense tectonics. Sediment deposits result locally deformed, likely because of differential sinking.

The volcanic seamount in the southern segment (Fig. 4) is located on a major extensional lineament and is interested by a normal fault, suggesting recent

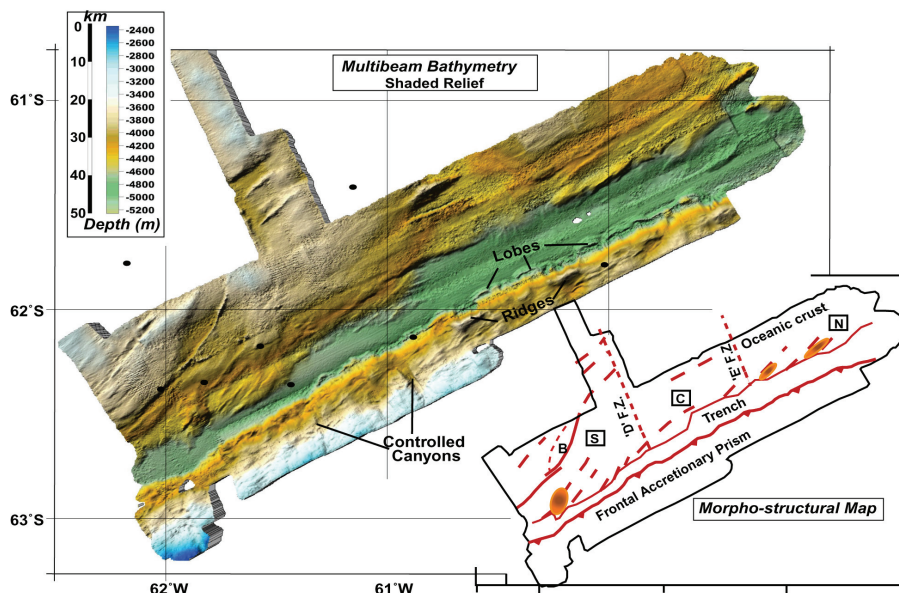


Figure 4. Shaded relief morpho-bathymetry of the investigated area. The schematic morpho-structural interpretation is shown. Solid orange ellipses indicate volcanic edifices; B=half graben. Black dots indicate the location of earthquakes, taken from the web site <http://epsc.wusl.edu/seismology/SEPA>.

tectonic activity following its emplacement. The seafloor morphology close to the volcano, combined with the positive magnetic anomaly, suggests that the activity is recent and favoured by extensional tectonics (Loreto et al., 2006). Two other seamounts, located in the Northern segment are oriented parallel to the oblique extensional lineaments (Fig. 4).

Oblique faults exhibit a significant throw at the seafloor, mainly in the SW oceanic segment (Fig. 2); it becomes less pronounced close to the trench axis and toward the outer rise (Fig. 4). The fault expression close to the trench is likely masked by sediment infill and by distal bottom current sedimentary deposits, as image to the SW of “D” FZ (fig. 3). On the other hand, the reduced throw toward the outer rise could be due to the less intense plate bending. Analysis of these geometrical features suggests that plate bending partially controls the activity of normal faults, as observed along the Costa Rica margin (Ranero et al., 2003). The smooth morphology of the Central segment is affected by few regular lineaments oriented orthogonally to the “D” and “E” FZs (Figs. 1b and 4). These structural and morphological characters abruptly change approaching the “D” and “E” FZs (figs. 3 and 4) suggesting that the FZs could act as mechanical discontinuities, reducing the coupling forces that might allow a larger bending of the Central segment. We speculate that the crustal thickness, related to the different age of each segment, cannot exhibit an appropriate depth-age relation, because of a significant change in the coupling at the “D” and “E” FZs, with respect to the PHO plate boundaries.

In the Southern and Northern segments the normal faults are at a different angle with the continental margin strike and do not appear to cut across the oceanic segment boundaries (Figs. 1 and 4), confirming that the FZs act as a mechanical boundary to the propagation of the deformation (Figs. 1b and 4). The extensional character of the oblique trending faults forms localized horst and graben structures (Kim et al., 1995) and suggests that the extension is produced by the plate bending and by inherited or pre-existing weak zones, as observed along other margins (Masson, 1991; Ranero et al., 2005). We hypothesize that the orientation of this normal faults system could be controlled by the different coupling along the transform faults; it is likely higher along Hero and Shackleton FZs and lower along “D” and “E” FZs, thus modifying the stress field orientation.

The analysis of new geophysical data acquired offshore the AP highlighted crustal structures affecting the PHO plate remnant and allowed to recognize differential passive subduction in the South Shetland trench. The incoming oceanic plate is affected by a recent normal fault system characterized by orientations ranging from parallel to oblique with respect to the trench axis and by volcanic activity. Horst and graben structures and basins are located in correspondence to these oblique lineaments. They are likely controlled by: (1) bending of the oceanic plate; (2) presence of inherited or pre-existing weak zones; (3) presence of mechanical discontinuities as the “D” and “E” Fracture Zones. Their different mechanical coupling could modify the stress field orientation within the PHO remnant.

Acknowledgements. We thank the editorial board for handling the manuscript and the officers and crew onboard the R/V OGS-Explora. F. Ferraccioli, D. Fontana and C.R. Ranero greatly contributed to the discussion. This work was supported by Italian Antarctic Program (PNRA).

References

- Barker P.F. (1982), The Cenozoic subduction history of the Pacific margin of the Antarctic Peninsula: Ridge crest-trench interactions, *Geol. Soc. London J.*, 139, 787-801.
- Carbotte S.M. and K.C. Macdonald (1994), Comparison of seafloor tectonic fabric at the intermediate, fast, and super fast spreading ridges: Influence of spreading rate, plate motions, and ridge segmentation on fault patterns, *J. Geophys. Res.*, 99, 13609-13631.
- Cohen J.K. and J.W. Stockwell Jr. (2003), CWP/SU: Seismic Unix Release 37: a free package for seismic research and processing, Centre for Wave Phenomena, Colorado School of Mines.
- Hawkes D.D. (1981), Tectonic segmentation of the northern Antarctic Peninsula, *Geology*, 9, 220-224.
- Kim Y., H.-S. Kim, R.D. Larter, A. Camerlenghi, L.A.P. Gambôa and S. Rudowski (1995), Tectonic deformation in the upper crust and sediments at the South Shetland Trench, In *Geology and Seismic Stratigraphy of the Atlantic Margin*, edited by A.K. Cooper, P.T. Barker and G. Brancolini, *Antarct. Res. Ser.*, 68, pp.157-166, AGU, Washington, DC.
- Kobayashi K., M. Nakanishi, K. Tamaki and Y. Ogawa (1998), Outer slope faulting associate with the western Kuril and Japan trenches, *Geophys. J. Int.*, 134, 356-372.
- Larter R.D. and P.F. Barker (1991), Effects of ridge crest-trench inter-action on Antarctic-Phoenix spreading: forces on a young subducting plate, *J. Geophys. Res.*, 96, 19583-19607.
- Lodolo E., A. Camerlenghi, G. Madrussani, U. Tinivella and G. Rossi (2002), Assessment of gas hydrate and free gas distribution on the South Shetland margin (Antarctica) based on multichannel seismic reflection data, *Geophys. J. Int.*, 148, 103-119.
- Loreto M.F., B. Della Vedova, F. Accaino, U. Tinivella, D. Accettella (2006), Shallow Geological structures of the South Shetland Trench, *Antarctic Peninsula, Offioliti*, 31(2), 151-159.
- Lawver L.A., R.A. Keller, M.R. Fisk, and J.A. Strelin (1995) Bransfield Strait, Antarctic Peninsula: Active extension behind a dead arc, in *Back arc basin: Tectonics and magmatism*, edited by B. Taylor, pp. 315-342, Amsterdam Plenum Press.
- Masson D.G. (1991), Fault patterns at outer trench walls, *Mar. Geophys. Res.*, 13, 209-225.
- Ranero C.R., J.P. Morgan, K. McIntosh and C. Reichert (2003), Bending-related faulting and mantle serpentinization at the Middle America trench, *Nature*, 425, 367-373.
- Ranero C.R., A. Villaseñor, J.P. Morgan and W. Weinrebe (2005), Relationship between bend-faulting at trenches and intermediate-depth seismicity, *Geoch. Geoph. Geosys.*, 6(12), Q12002, doi:10.1029/2005GC000997.
- Robertson Maurice S.D., D.A. Wiens, P.J. Shore, E. Vera and R. M. Dorman (2003) Seismicity and tectonics of the South Shetland Islands and Bransfield Strait from a Regional broadband seismograph deployment, *J. Geophys. Res.*, 108 (B10), 2461, doi:10.1029/2003JB002416.
- Sandwell D.T. and W.H.F. Smith (1997), Marine gravity anomaly from Geosat and ERS-1 satellite altimetry, *J. Geophys. Res.*, 102(5), 10039-10054.
- Scholl D.W., M.N. Christensen, R. von Huene, and M.S. Marlow (1970) Peru-Chile trench sediments and sea-floor spreading, *Geol. Soc. of Am. Bull.*, 81, 1339-1360.
- von Huene R. and C.R. Ranero (2003) Subduction erosion and basal friction along the sediment starved convergent margin off Antofagasta, Chile, *J. Geophys. Res.*, 108: 2079, doi:10.1029/2001JB001569.